applied sciences

MDPI

Article

Formation of Water-Soluble Fluorescent Fractions During Thermal Processing of β-Glucan-Rich Medicinal Mushrooms

Gréta Törős [1,2,*], Reina Atieh [3,4], Aya Ferroudj [1,2], Dávid Semsey [1,4], Florence Alexandra Tóth [5], Péter Tamás Nagy [5] and József Prokisch [1]

[1] Institute of Animal Science, Biotechnology and Nature Conservation, Faculty of Agricultural and Food Sciences and Environmental Management, University of Debrecen, Böszörményi Street 138, 4032 Debrecen, Hungary; ferroudj.aya@agr.unideb.hu (A.F.); semi@gmail.hu (D.S.); jprokisch@agr.unideb.hu (J.P.)
[2] Doctoral School of Animal Husbandry, Faculty of Agricultural and Food Sciences and Environmental Management, University of Debrecen, Böszörményi Street 138, 4032 Debrecen, Hungary
[3] Institute of Agricultural Chemistry and Soil Science, Faculty of Agricultural and Food Sciences and Environmental Management, University of Debrecen, 138 Böszörményi Street, 4032 Debrecen, Hungary; atieh.reina@mailbox.unideb.hu
[4] Doctoral School of Nutrition and Food Science, University of Debrecen, Böszörményi Street 138, 4032 Debrecen, Hungary
[5] Institute of Water and Environmental Management, Faculty of Agricultural and Food Sciences and Environmental Management, University of Debrecen, Böszörményi Street 138, 4032 Debrecen, Hungary; toth.florence@agr.unideb.hu (F.A.T.); nagypt@agr.unideb.hu (P.T.N.)
* Correspondence: toros.greta@agr.unideb.hu

Abstract

Thermal processing of biomass can induce chemical transformations that lead to the formation of fluorescent carbonaceous products. In this study, six β-glucan-rich medicinal mushrooms, *Ganoderma lucidum*, *Cordyceps sinensis*, *Inonotus obliquus*, *Lentinula edodes*, *Grifola frondosa*, and *Hericium erinaceus*, were subjected to mild pyrolytic treatment (200 °C for 3 h) to investigate the formation of water-soluble fluorescent fractions. Physicochemical characterization of aqueous extracts was performed using high-performance liquid chromatography size-exclusion chromatography (HPLC-SEC), fluorescence emission spectroscopy, Fourier-transform infrared spectroscopy (FTIR), and β-glucan quantification. Fluorescence emission spectra revealed species-dependent differences in emission intensity, with the most pronounced signals observed for *G. lucidum* and *C. sinensis*. HPLC-SEC analysis showed only minor changes in molecular weight distribution after thermal treatment, suggesting limited polymer degradation. FTIR spectra indicated moderate structural modifications consistent with partial carbonization and chemical rearrangement within the mushroom matrices. Despite the mild processing conditions, measurable increases in fluorescence intensity were observed in several species, indicating the formation of fluorescent carbon-rich molecular structures. These findings demonstrate that moderate thermal treatment of β-glucan-rich fungal biomass can generate water-soluble fluorescent carbonaceous fractions without extensive breakdown of the original polysaccharide matrix. The results provide new insights into thermally induced photophysical changes in medicinal mushrooms and contribute to understanding the formation of fluorescent carbonaceous products from natural biomaterials.

Keywords: fluorescent carbonaceous fractions; thermal processing; medicinal mushrooms; mushroom biomass; β-glucans; fluorescence spectroscopy

Academic Editor: Antonios E. Koutelidakis

Received: 12 March 2026
Revised: 14 April 2026
Accepted: 14 April 2026
Published: 17 April 2026

1. Introduction

Carbon-based fluorescent materials are widely investigated due to their photoluminescence, biocompatibility, and tunable surface chemistry [1,2]. These qualities enable their application in fluorescence-based sensing, imaging, drug delivery, and environmental detection [2,3]. The emerging field of "myco-nanotechnology" utilizes medicinal mushrooms, rich in proteins, sugars, and β-glucan, as eco-friendly, sustainable, naturally sourced materials for the synthesis of nanomaterials. The mild thermal treatment of mushroom biomass produces water-dispersible, water-soluble fluorescent fractions [4]. In this study, we focus on water-soluble fluorescent carbonaceous fractions obtained after mild thermal treatment; direct nanoscale imaging and isolation of discrete nanoparticles were not performed.

Recent advancements in nanomaterial fabrication have increasingly prioritized the development of sustainable, green synthesis methodologies [1–3]. Consequently, "myco-nanotechnology" an interdisciplinary approach integrating mycology and nanotechnology has emerged as a highly promising avenue [4,5]. This paradigm utilizes edible and medicinal mushrooms as renewable, eco-friendly precursors for nanomaterial production. Mushrooms possess a rich matrix of biologically active compounds, such as amino acids and sugars, which serve as optimal carbon sources. Through controlled mild thermal treatment in the absence of oxygen, these organic precursors undergo carbonization and Maillard reactions to yield water-dispersible, fluorescent carbonaceous fractions, aligning closely with global sustainability objectives [6,7]. Amino acids and reducing sugars are particularly suitable precursors because their Maillard-driven condensation forms nitrogen-containing heteroaromatic intermediates that act as carbonization nuclei and enable intrinsic nitrogen incorporation into the developing carbon framework [8,9].

β-Glucan represents a major bioactive component of medicinal mushrooms and is widely recognized for its immunomodulatory, antioxidant, and antineoplastic activities [10–12]. Structurally, β-glucans are polysaccharides primarily composed of β-(1→3) and β-(1→6) glycosidic linkages, whose branching architecture and high hydroxyl group density may significantly influence thermal dehydration and carbonization pathways [13]. Previous studies have demonstrated that the molecular structure and functional group distribution of polysaccharide precursors strongly affect nucleation, aromatization, and graphitization processes during hydrothermal or pyrolytic treatment, ultimately determining the size, surface chemistry, and optical properties of the resulting carbon-based nanomaterials [14,15]. Biomass-derived carbon-rich products have attracted considerable attention due to their sustainability, low toxicity, and tunable photoluminescent characteristics [15,16]. However, despite the prevalence of β-glucan in fungal biomass, its specific mechanistic contribution to the formation and property modulation of carbon-based nanomaterials remains insufficiently elucidated. Establishing a correlation between β-glucan content and the physicochemical characteristics of the synthesized carbon-based nanomaterials would clarify structure–property relationships and enable rational precursor selection and process optimization [14,17]. From an industrial perspective, such insights could facilitate the development of sustainable, biomass-derived carbon-based nanomaterials with controllable optical performance, supporting scalable and cost-effective production strategies for applications in bioimaging, sensing, and functional coatings [18].

Our research aims to investigate how the biochemical composition of different medicinal mushroom matrices, with particular emphasis on their β-glucan content, relates to the formation and properties of water-soluble fluorescent carbonaceous fractions generated during mild thermal treatment. In this context, β-glucan was considered primarily as a structural and compositional biomarker of the original mushroom matrix rather than as a directly measured component of the fluorescent fractions. The selected mushrooms for this study include well-known species such as *Ganoderma lucidum* (reishi), *Cordyceps sinensis*

(caterpillar fungus), *Inonotus obliquus* (chaga), *Lentinula edodes* (shiitake), and *Grifola frondosa* (maitake), all of which are characterized by distinct biochemical profiles and established therapeutic applications [19–23].

Overall, our focuses on the characterization of water-soluble fluorescent carbonaceous fractions generated during controlled mild thermal processing of mushroom biomass.

The main objectives of this study are:

1. To evaluate the feasibility of producing water-soluble fluorescent carbonaceous fractions from commercially available medicinal mushroom biomass via controlled mild thermal treatment.
2. To quantify the β-glucan content of the selected mushroom species and explore potential indirect relationships between matrix composition and the fluorescence characteristics of the resulting carbonaceous fractions.

2. Materials and Methods

2.1. Sample Selection and Thermal Treatment

In our previous work, we demonstrated that mild thermal treatment of *Pleurotus ostreatus* powders at temperatures between 150–240 °C produces water-soluble fluorescent carbon fractions, with potential antioxidant and bioactive properties [6]. However, the influence of mushroom-derived bioactive compounds, particularly β-glucans, on the formation and fluorescence of carbonaceous fractions remains underexplored. This study investigates how six β-glucan-rich medicinal mushrooms can serve as natural sources for fluorescent carbon fractions with distinct optical and chemical properties.

For this study, commercially available medicinal mushroom powders: *Cordyceps sinensis* (caterpillar fungus), *Ganoderma lucidum* (reishi), *Grifola frondosa* (maitake), *Hericium erinaceus* (lion's mane), *Inonotus obliquus* (chaga), and *Lentinula edodes* (shiitake)—were procured from Varga Reformház Ltd. (Debrecen, Hungary, BioMenü brand).

All powders were subjected to dry mild thermal treatment at 200 °C for 3 h in sealed ceramic crucibles to prevent oxidation, based on prior optimization studies [10]. Both the pyrolyzed and unprocessed powders were analyzed, resulting in 12 experimental groups (Figure 1).

Figure 1 provides a photographic overview of the fresh fruiting bodies, commercially available powders, initial powders, and mild thermal-treated materials of the six mushroom species.

2.2. Characterization of Fluorescent Carbonaceous Fractions

2.2.1. Sample Preparation

For each mushroom species, 10 g of powder was subjected to dry mild thermal treatment at 200 °C for 3 h in sealed ceramic crucibles to prevent oxidation. Immediately after processing, the charred residues were suspended in 50 mL of deionized water and sonicated at 40 kHz for 30 min to facilitate the release and dispersion of water-soluble fluorescent carbonaceous fractions. The suspensions were subsequently filtered through a 0.22 µm membrane to remove insoluble particles. The obtained filtrates remained visibly stable without precipitation or phase separation, indicating that the fluorescent components were present in the water-dispersible fraction. The resulting solutions were then freeze-dried for subsequent analyses, including fluorescence spectroscopy, FTIR, and β-glucan content determination.

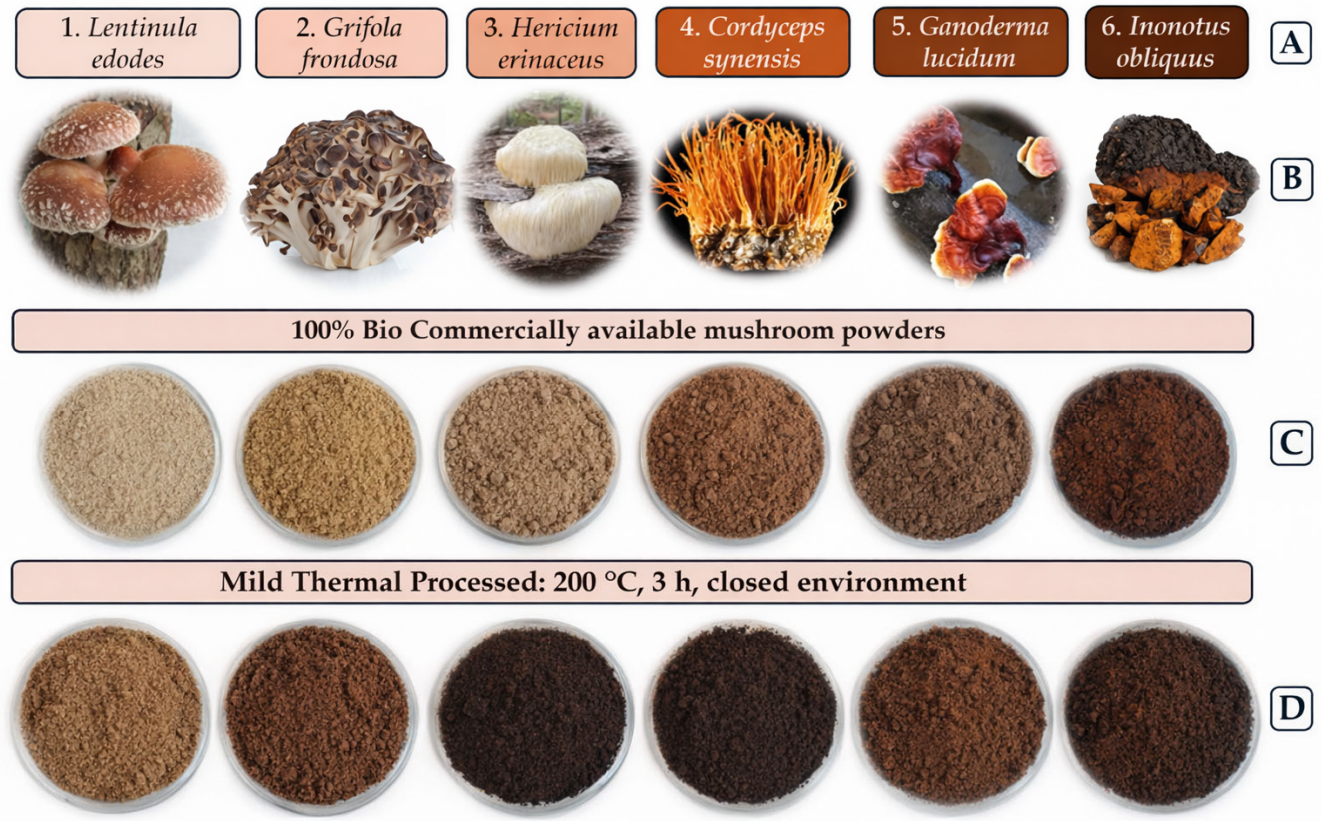

Figure 1. Photographic illustration of mushroom samples from the fresh fruiting body into mild thermal-treated mushroom powders. (**A**) Latin name of the selected mushroom; (**B**) Pictures from the fresh mushroom; (**C**) Commercially available mushroom powders; (**D**) Mild-thermal processed mushroom.

2.2.2. HPLC-SEC Analysis

Molecular weight distribution and polydispersity of the fluorescent carbonaceous fractions were determined by high-performance liquid chromatography coupled with size-exclusion chromatography and fluorescence detection (HPLC-SEC-FLD). Separation was employed on an Agilent AdvanceBio SEC column (4.6 × 300 mm, 2.7 µm, 300 Å) with the Shimadzu RF-20A fluorescence detector. The mobile phase composition was 20% acetonitrile in water (v/v) at a flow rate of 0.7 mL/min.

Sample injection volume was 5 µL, with excitation and emission wavelengths set at 370 nm and 460 nm, respectively. Calibration was performed using peptide standards (Bio-Rad, Merck, Darmstadt, Germany) and synthetic carbon nanodots (CND) references as described by Nguyen et al. (2024) and as mentioned at Figure 2 (Standard Sample-Pure CND) [24]. Polydispersity index (PDI) was calculated as the Mw/Mn ratio.

In this study, the results from the investigation of "carbonaceous fractions" inferred from spectroscopic and HPLC-SEC-FLD behavior relative to a previously characterized reference material; however, while our samples were not physically isolated or directly imaged, and definitive nanoscale morphology was not confirmed.

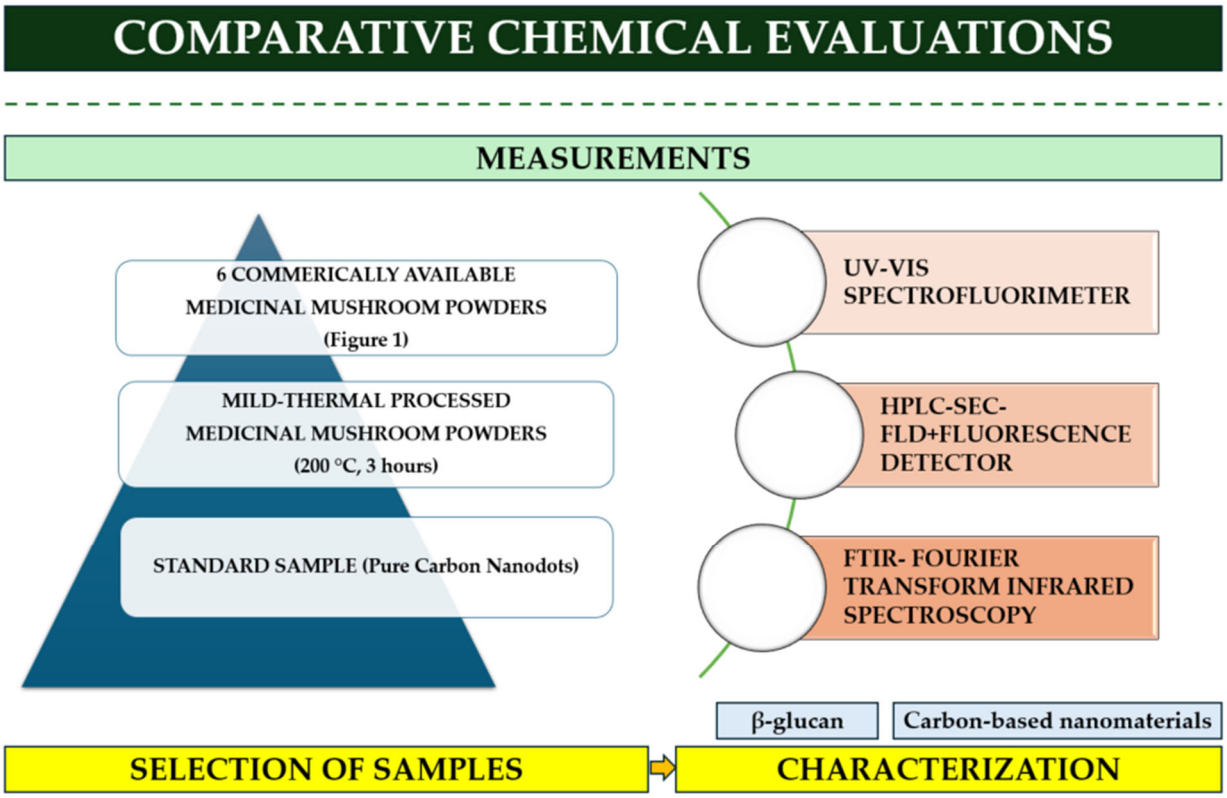

Figure 2. Summarization of the research protocol, including the performed analytical chemical tests with selected mushrooms from the treated and untreated mushroom groups and the standard sample.

2.2.3. Fluorescence Spectroscopy

The fluorescence characteristics of water-soluble fluorescent carbonaceous fractions derived from medicinal mushrooms were examined using an RF-1501 Shimadzu spectrofluorometer (Shimadzu Corporation, Kyoto, Japan). Before measurement, all samples were re-dissolved in deionized water at a concentration of 2 mg/mL, filtered through a 0.22 µm membrane filter, and equilibrated to room temperature. Fluorescence emission spectra were recorded in the 400–800 nm range with a fixed excitation wavelength of 360 nm, based on pre-experiments that identified this wavelength as optimal for excitation of mushroom-derived fluorophores. Each measurement was performed in quartz cuvettes (1 cm path length). Background correction was applied using solvent blanks (deionized water). Fluorescence data were processed and visualized in Python (version 3.12) using the Pandas (version 2.2), NumPy (version 1.26), and Matplotlib (version 3.8) libraries.

2.2.4. FTIR Spectroscopy

The surface chemistry of the water-soluble fluorescent carbon fractions was analyzed using Fourier-transform infrared spectroscopy (FTIR) with an Agilent 4300 Handheld FTIR spectrometer equipped with an ATR (attenuated total reflectance) accessory. Samples were measured directly on the ATR crystal without further preparation. Spectra were recorded over the 4000–650 cm^{-1} range at a 4 cm^{-1} resolution. Background spectra were collected before each measurement, and the ATR crystal was cleaned between samples. The resulting spectra were baseline-corrected, normalized, and examined for changes in key functional groups associated with the mild thermal treatment process.

It should be mentioned that Temperature-dependent FTIR (FTIR-T) analysis was performed to assess the thermal stability and degree of carbonization of the synthesized nanodots. The gradual attenuation of O–H and C–O stretching bands with increasing temperature supports the transformation of polysaccharide precursors into a fluorescent

carbonized structure, supporting progressive dehydration and chemical transformation consistent with partial carbonization.

2.3. Bioactive Compound Quantification

β-Glucan Content

β-Glucan content was determined using the Megazyme Mushroom and Yeast β-Glucan Assay Kit (Megazyme International, Bray, Ireland), based on enzymatic hydrolysis and spectrophotometric quantification according to the manufacturer's protocol [25]. Quantification was expressed as milligrams per gram of dry weight and compared across all species before and after mild thermal treatment. It should be mentioned that β-Glucan content was determined in the original and mild-thermally treated whole-mushroom powders, not in the isolated fluorescent carbonaceous fractions.

The purpose of this measurement was to characterize the biochemical composition of the initial mushroom matrices and to evaluate whether differences in β-glucan content among species may relate indirectly to the formation and fluorescence behavior of the dissolved carbonaceous fractions generated during thermal processing.

In this context, β-glucan was used as a compositional indicator of the precursor matrix rather than as a constituent directly measured within the fluorescent fractions.

2.4. Statistical Analysis

Outliers were screened prior to testing normality using the Shapiro–Wilk test. Parametric data were analyzed by one-way ANOVA followed by Tukey's post hoc test, whereas nonparametric data were evaluated using the Kruskal–Wallis test with Dunn's post hoc comparison (Polydisperse Intensity, Molecular weight, Fluorescence intensity). All measurements were performed in triplicate as technical replicates derived from the same batch of mushroom material; therefore, statistical comparisons should be interpreted as analytical variability rather than biological variation. Thus, the replicates reflect analytical repeatability rather than independent biological variation between batches. Treated groups were statistically compared to their respective untreated control groups. Data visualization and correlation analyses were performed using Microsoft Excel (365 Edition), and statistical analyses were conducted with SPSS version 25.0. Statistical significance was set at $p < 0.05$.

3. Results

3.1. Structural Characterization

3.1.1. Molecular Weight and Polydisperse Intensity

HPLC was used to evaluate the molecular characteristics of mushroom powders, both raw and pyrolyzed, as shown in Table 1. All treatments were standardized to 10 g of dry mushroom powder per sample. Weight-average molecular weight (Mw) was determined from retention times and calibration curves, and polydispersity (PD%) was calculated to assess the uniformity of the molecular size distribution. From the Mw and PD values, the number-average molecular weight (Mn) was derived (Mn = Mw/PD). No statistically significant differences ($p > 0.05$) were observed in molecular weight and PD between untreated and pyrolyzed samples for any of the tested mushroom species. The consistency of the data suggests that mild thermal treatment, under the applied conditions, does not substantially alter the molecular structure of the main macromolecular components. The calculated Mn values further support this conclusion. While Mn reflects a greater sensitivity to low-molecular-weight fractions, it remained relatively stable across conditions, showing no systematic shifts attributable to the treatment. The PD values, which quantify distribution breadth, stayed within a moderate range across most samples, indicating comparable molecular heterogeneity between the raw and pyrolyzed forms. Overall, the

molecular profiling data suggest that the polysaccharide content remains structurally stable during mild thermal treatment, with no detectable fragmentation or aggregation under the tested conditions.

Table 1. Molecular weight (kDa) and Polydispersity Intensity (PD%) of medicinal mushroom powders pyrolyzed at one specific temperature (200 °C) for a time duration (3 h).

Name of the Sample	Molecular Weight (kDa)	PD%
lion's mane	588 ± 47	5.11 ± 0.11
P_lion's mane	621 ± 24	4.65 ± 0.12
shiitake	611 ± 9	4.23 ± 0.78
P_shiitake	665 ± 27	4.83 ± 0.01
caterpillar fungus	642 ± 49	5.23 ± 1.60
P_caterpillar fungus	664 ± 44	4.86 ± 0.23
maitake	637 ± 48	4.87 ± 0.24
P_maitake	658 ± 32	4.60 ± 0.43
reishi	679 ± 44	4.65 ± 0.93
P_reishi	672 ± 16	4.12 ± 0.91
chaga	642 ± 55	2.71 ± 0.18
P_chaga	630 ± 36	2.59 ± 0.14

Values are shown as the mean ± SD. No significant differences between samples ($p > 0.05$).

3.1.2. Fluorescence Intensity

The fluorescence intensity of water-soluble fluorescent carbon fractions was measured, and the total intensities of samples with higher and lower peak heights were analyzed, with differentiation based on their dimerization states. Chromatographic analysis revealed variations in peak patterns across samples. In all cases, three distinct peaks were consistently observed in both pyrolytically processed and unprocessed forms. An exception was noted in the chaga samples (both chaga and P_chaga), where only two peaks were detected. Pairwise comparisons were conducted between pyrolytically processed and unprocessed samples for each mushroom species. Statistically significant differences ($p < 0.05$) were identified between the commercially available samples and those subjected to pyrolytic processing. Comparative fluorescence intensity profiles for all investigated mushroom species are summarized in Figures 3 and 4.

In lion's mane, fluorescence intensity was increased from 71 to 255 A.u. ($p = 0.006$, +259%). The most pronounced enhancement was observed in shiitake, where the value rose from 26 to 110 A.u. ($p = 0.001$, +323%). The chromatogram for shiitake is shown in Figure 4. A substantial increase was also recorded for maitake, from 74 to 224 A.u. ($p = 0.001$, +203%). In reishi, a more moderate yet statistically significant increase was measured, from 21 to 38 A.u. ($p = 0.015$, +81%).

In the case of chaga, fluorescence was found to increase from 30 to 68 A.u. ($p = 0.020$, +127%), although the effect was less pronounced than in other species.

By contrast, a marked decrease was recorded for caterpillar fungus, with fluorescence intensity dropping from 209 to 103 A.u. ($p = 0.020$, −51%). It was demonstrated that the fluorescence intensity of mushroom powders can be enhanced through pyrolytic processing. However, this enhancement was not consistent across all species, as evidenced by the significant reduction observed in caterpillar fungus.

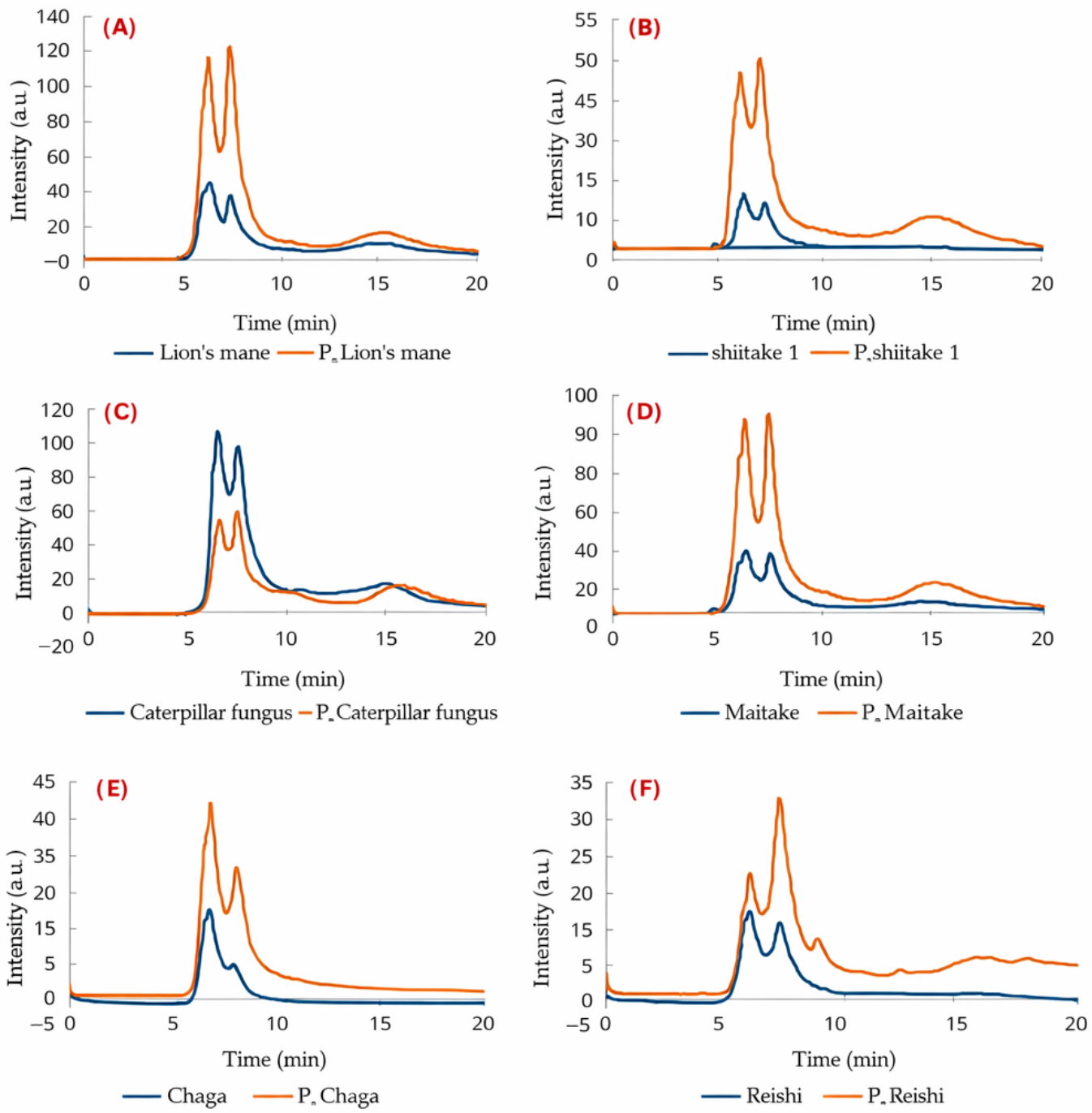

Figure 3. Representative fluorescence chromatogram obtained by HPLC-SEC-FLD analysis of *Lentinula edodes* (shiitake) samples before and after mild thermal treatment. The comparison illustrates the increase in fluorescence intensity observed in the thermally treated sample ("_P"). Fluorescence detection was performed at an excitation wavelength of 360 nm and emission monitoring across the 400–800 nm range. The chromatogram highlights the presence of water-soluble fluorescent carbonaceous fractions formed during thermal processing in the case of different mushroom species: (**A**)—Lion's mane, (**B**)—Shiitake, (**C**)—Caterpillar fungus, (**D**)—Maitake, (**E**)—Chaga, (**F**)—Reishi.

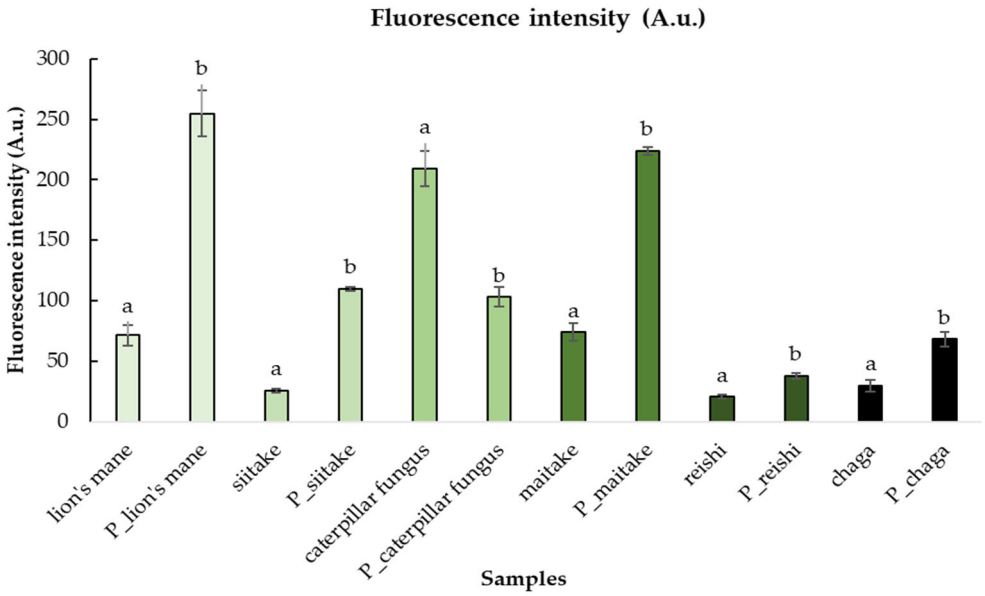

Figure 4. Fluorescence intensity (A.u.) of mushroom powders pyrolyzed at one specific temperature (200 °C) for a time duration (3 h). Significant differences are indicated by different letters (a, b).

3.1.3. Fluorescence Emission Spectra (Ex = 360 nm)

Figure 5 presents fluorescence emission data in the form of heatmaps for native and thermally processed ("_P") mushroom powders. In these heatmaps, the x-axis represents the emission wavelength range (400–800 nm), the y-axis corresponds to the different mushroom species, and the color scale indicates fluorescence intensity (A.U.). This visualization enables comparison of species-dependent intensity distributions across the emission spectrum.

The results reveal broad and overlapping emission features characteristic of complex biomass-derived fluorescent systems. Therefore, species-specific differences are primarily reflected in the distribution and intensity of emission rather than sharp or well-separated spectral peaks.

Hericium erinaceus (lion's mane) and *Lentinula edodes* (shiitake) exhibited dominant emission in the near-UV/blue region (~400–480 nm), with a slight reduction in overall fluorescence intensity after thermal treatment. *Cordyceps sinensis* (caterpillar fungus), *Grifola frondosa* (maitake), and *Inonotus obliquus* (chaga) showed similar primary emission around ~400 nm, with minor increases in longer wavelength regions (600–800 nm) after processing. In contrast, *Ganoderma lucidum* (reishi) displayed a characteristic emission maximum around ~440 nm and a noticeable increase in fluorescence intensity following thermal treatment, which fact can be attributed to the formation of carbonized nanostructures with increased conjugated π-domains and surface defect states during pyrolysis, which enhance radiative recombination and thus fluorescence emission.

Overall, mild thermal processing led to a redistribution of fluorescence intensity across the emission range rather than significant shifts in peak position, suggesting modifications in the composition and structure of fluorescent carbonaceous components.

3.2. The Results of FTIR Analysis

Figure 6 presents the FTIR spectra of commercially available dried medicinal mushroom powders before and after mild thermal treatment at 200 °C for 3 h, revealing species-specific chemical changes induced by thermal treatment.

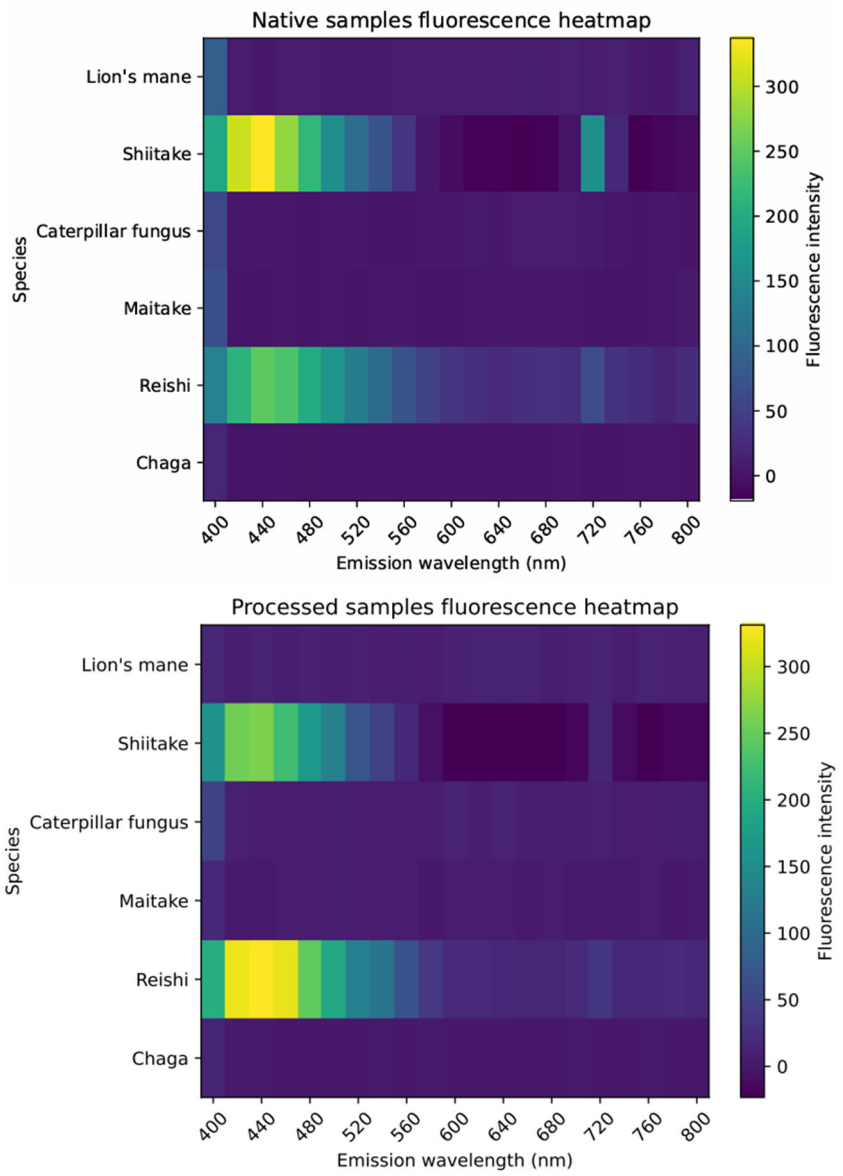

Figure 5. Fluorescence emission heatmaps of native and thermally processed ("_P") mushroom powders recorded at an excitation wavelength of 360 nm. The x-axis shows emission wavelength (400–800 nm), the y-axis represents mushroom species, and the color scale indicates fluorescence intensity (A.U.). The heatmaps illustrate species-dependent intensity patterns and changes induced by mild thermal treatment.

Cordyceps sinensis exhibited pronounced chemical transformations following mild thermal treatment. The FTIR spectra showed a significant decrease in the intensity of broad O–H and N–H stretching bands, indicative of dehydration and loss of hydroxyl and amine groups. Additionally, the C–H stretching bands corresponding to alkyl groups were markedly reduced, reflecting thermal degradation of these moieties. New absorption peaks assigned to carbonyl groups emerged, suggesting structural rearrangement and oxidation of polysaccharides and proteins during mild thermal treatment.

In contrast, *Ganoderma lucidum* demonstrated exceptional thermal stability. The FTIR profiles of the original and pyrolyzed powders were nearly identical, with negligible changes across all characteristic bands. This indicates that the molecular structures of *Ganoderma lucidum's* biomacromolecules are primarily resistant to chemical modifications under the applied pyrolytic conditions.

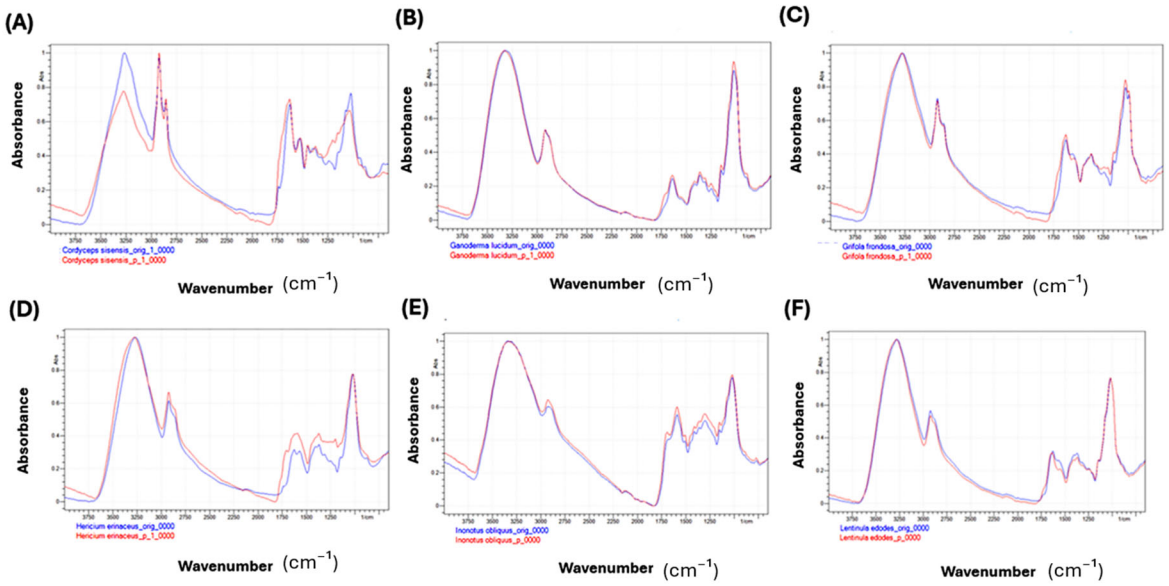

Figure 6. FTIR spectra of six medicinal mushroom powders before (1, blue) and after (2, red) mild thermal treatment (200 °C, 3 h). Comparative FTIR spectra of *Cordyceps sinensis* (**A**), *Ganoderma lucidum* (**B**), *Grifola frondosa* (**C**), *Hericium erinaceus* (**D**), *Inonotus obliquus* (**E**), and *Lentinula edodes* (**F**), showing treatment-induced changes in functional groups, including hydroxyl, amine, alkyl, and carbonyl regions.

Grifola frondosa showed only slight chemical changes after mild thermal treatment. The hydroxyl and amine group peaks exhibited a minor decrease in intensity, while subtle shifts appeared in the fingerprint region (1500–1000 cm^{-1}) and carbonyl-related bands. These spectral observations suggest mild dehydration and limited structural modifications, with the primary biomolecular framework remaining largely intact.

For *Hericium erinaceus*, the principal absorption bands remained largely preserved after thermal treatment. In the 3300–3500 cm^{-1} region, only minor spectral variations were observed rather than a clear intensity decrease. In contrast, more distinct changes were detected in the fingerprint region, suggesting structural modifications induced by pyrolysis.

These patterns suggest that mild thermal treatment led to partial dehydration and some restructuring of functional groups within polysaccharides and proteins, resulting in moderate molecular alterations.

Similarly, *Inonotus obliquus* powders retained their key chemical signals after mild thermal treatment, with FTIR spectra showing comparable major absorption bands before and after treatment. However, the pyrolyzed sample showed reduced intensities of the O–H/N–H stretching bands and mild changes in the fingerprint region, indicating mild dehydration and structural reorganization. Thus, mild thermal treatment caused partial decomposition and transformation of functional groups while preserving much of the mushroom's molecular architecture. *Lentinula edodes* showed minimal chemical changes after mild thermal treatment. Its FTIR spectra before and after treatment were highly similar, with only a slight decrease in the O–H/N–H stretching region and negligible alterations in the fingerprint region. This implies that the pyrolytic process induced only mild dehydration and subtle structural changes, maintaining most of the mushroom's fundamental chemical structures and functional groups.

3.3. The Comparison of Peak Height Ratio and Peak Area Ratio

Quantitative evaluation of baseline-corrected FTIR peak height and peak area ratios, normalized to the 1030 cm^{-1} polysaccharide band, proposed species-dependent chemical modifications induced by mild thermal treatment. The most pronounced changes were

observed for *C. sinensis* and *H. erinaceus*, which exhibited substantial increases in the carbonyl index, indicating oxidation and formation of new C=O functionalities. In contrast, G. lucidum showed only minor variations across most spectral regions, supporting its higher thermal stability. Chaga displayed moderate carbonyl enhancement, while Shiitake and Maitake exhibited only limited dehydration-related modifications. These quantitative findings are consistent with the qualitative spectral observations and further substantiate the differential thermal response of β-glucan-rich mushroom matrices. The calculated data are presented in Table 2.

Ms. Eris Zhang.

Table 2. Relative changes (Δ%) in baseline-corrected FTIR peak ratios after mild thermal treatment (untreated, Raw → pyrolyzed, P).

Species	ΔOH (H)	ΔCH (H)	ΔC=O (H)	Δ1600 (H)	ΔOH (A)	ΔCH (A)	ΔC=O (A)	Δ1600 (A)
Lion's mane	+7%	−4%	+369%	−57%	+8%	−6%	+649%	−86%
Shiitake	+11%	−1%	~0	~0	+15%	+5%	~0	~0
Caterpillar fungus	+98%	+192%	appeared	+157%	+100%	+108%	appeared	~0
Maitake	+17%	+6%	appeared	~0	+17%	+10%	~0	~0
Reishi	−10%	−13%	appeared	~0	−12%	−8%	appeared	~0
Chaga	~0	+4%	+65%	+4%	−2%	+3%	+89%	+7%

Δ% (Raw → P) represents the relative percentage change calculated as Δ% = ((P − Raw)/Raw) × 100. Positive values indicate an increase and negative values indicate a decrease after thermal treatment. Peak Height Ratio (H) represents the normalized maximum absorbance of a selected band relative to the 1030 cm^{-1} polysaccharide reference band, while Peak Area Ratio (A) corresponds to the integrated area of the same spectral region normalized to the same reference band. The analyzed regions include O–H/N–H stretching (3200–3400 cm^{-1}), C–H stretching (2800–3000 cm^{-1}), carbonyl vibrations (~1700 cm^{-1}), and the ~1600 cm^{-1} amide region.

3.4. Thermal-Induced Structural and Molecular Modifications in Medicinal Mushrooms Revealed by Fluorescence, FTIR, and β-Glucan Analyses

Controlled mild thermal treatment (200 °C, 3 h) of six commercially available medicinal mushroom powders induced species-specific structural and molecular modifications, as revealed by fluorescence spectroscopy, FTIR analysis, and β-glucan quantification. Although HPLC molecular weight profiles (Mw, Mn, PD%) remained largely unchanged, indicating preservation of major polysaccharide macromolecules, complementary spectroscopic analyses provide evidence of species-dependent chemical and photophysical modifications consistent with partial carbonization and formation of fluorescent carbonaceous products.

Fluorescence measurements (excitation at 360 nm, emission 400–800 nm) demonstrated distinct species-dependent responses (Table 3). Lion's mane exhibited a marked decrease in blue emission (~400 nm) with red-shifted broadening (600–740 nm), reflecting partial degradation and rearrangement of aromatic and protein-derived fluorophores. Shiitake showed moderate emission decreases, whereas Reishi and Chaga displayed enhanced fluorescence, indicative of formation of new conjugated structures. Caterpillar fungus and Maitake exhibited intermediate behaviors, consistent with partial fluorophore modification.

FTIR analysis revealed that thermal treatment caused measurable but variable chemical changes across species. *C. sinensis* showed pronounced reductions in O–H and N–H stretching bands and the appearance of new carbonyl absorptions, reflecting dehydration, oxidation, and molecular rearrangement. In contrast, *G. lucidum* and *L. edodes* remained largely unaltered, suggesting high thermal resilience. *G. frondosa*, *H. erinaceus*, and *I. obliquus* displayed mild to moderate changes, indicating partial structural reorganization while retaining overall polysaccharide integrity.

Table 3. Summary of proposed spectral changes in medicinal mushroom powders before and after pyrolytic treatment (200 °C, 3 h).

Mushroom Species	Fluorescence (Ex = 360 nm, 400–800 nm Range)	FTIR Spectral Observations	Proposed Interpretation	β-Glucan (% *w*/*w* for Dry Matter)
Lion's mane	Strong decrease in blue emission (~400 nm); red-shifted broadening toward 600–740 nm	Slight reduction of O–H/N–H stretching; minor changes in fingerprint region	Partial dehydration and moderate structural reorganization	↑ From 28.8 to 36.0
Shiitake	Decreased emission intensity (400–480 nm); loss of weak feature at ~720 nm	Minimal spectral change; slight decrease in O–H/N–H region	Mild dehydration; structure largely preserved	↑ From 34.05 to 37.1
Caterpillar fungus	Decrease at 400–500 nm; increased emission in 600–800 nm range	Marked decrease of O–H/N–H and C–H bands; new carbonyl peaks	Pronounced oxidation and molecular rearrangement	↑ From 28.9 to 33.9
Maitake	Lower emission at 400 nm; minor enhancement around 500–600 nm	Small intensity decrease in O–H/N–H region; slight shift in fingerprint area	Limited dehydration and mild modification	~Constant (~36.25%)
Reishi	Increased fluorescence, especially at 420–460 nm	Negligible spectral changes before/after mild thermal treatment	High chemical stability under applied conditions	↓ From 54.2 to 36.6
Chaga	Higher intensity at 400 nm and 700 nm after processing	Small decrease in O–H/N–H intensity; overall spectrum unchanged	Slight dehydration; overall structure retained	↑ From 28.1 to 36.7

β-Glucan content provided an additional biomarker to interpret these modifications. Apparent increases in Lion's mane, Shiitake, Chaga, and Maitake are likely due to relative concentration effects after water loss and enhanced extractability of polysaccharides, rather than new biosynthesis. Reishi exhibited a decrease in β-glucan content, consistent with partial thermal degradation. These observations confirm that species-specific glucan content and structure influence thermal stability and molecular rearrangements during mild thermal treatment.

Integration of fluorescence, FTIR, and β-glucan data suggests the formation of fluorescent carbonaceous products derived from thermally modified mushroom matrices. Mushrooms with highly ordered β-(1→3)-glucan backbones and minimal side-branching (*G. lucidum*, *L. edodes*) maintained structural integrity with moderate fluorescence changes, whereas species with more amorphous or protein-associated glucans (*C. sinensis*, Lion's mane) underwent extensive rearrangements, resulting in altered fluorophore properties. Chaga and Maitake exhibited moderate structural modifications, accompanied by increased relative β-glucan availability.

Overall, these results highlight that mild thermal treatment at moderate temperatures likely promotes partial carbonization and the formation of fluorescent carbon-rich domains. The combination of spectroscopic, molecular, and biochemical analyses provides a robust and multi-dimensional understanding of how β-glucan-rich mushroom matrices contribute to the formation and functional properties of carbonaceous fractions.

Figure 7 illustrates the relative changes in fluorescence intensity and FTIR-derived structural modifications for six medicinal mushroom powders subjected to controlled mild thermal treatment. Fluorescence variation is represented by blue bars: negative values indicate decreased emission intensity near 400 nm (blue fluorophores), while positive values denote enhanced or red-shifted emission associated with formation of more conjugated structures. FTIR variation, depicted in light blue, quantifies the degree of structural change inferred from O–H/N–H stretching reductions and emergence of carbonyl bands.

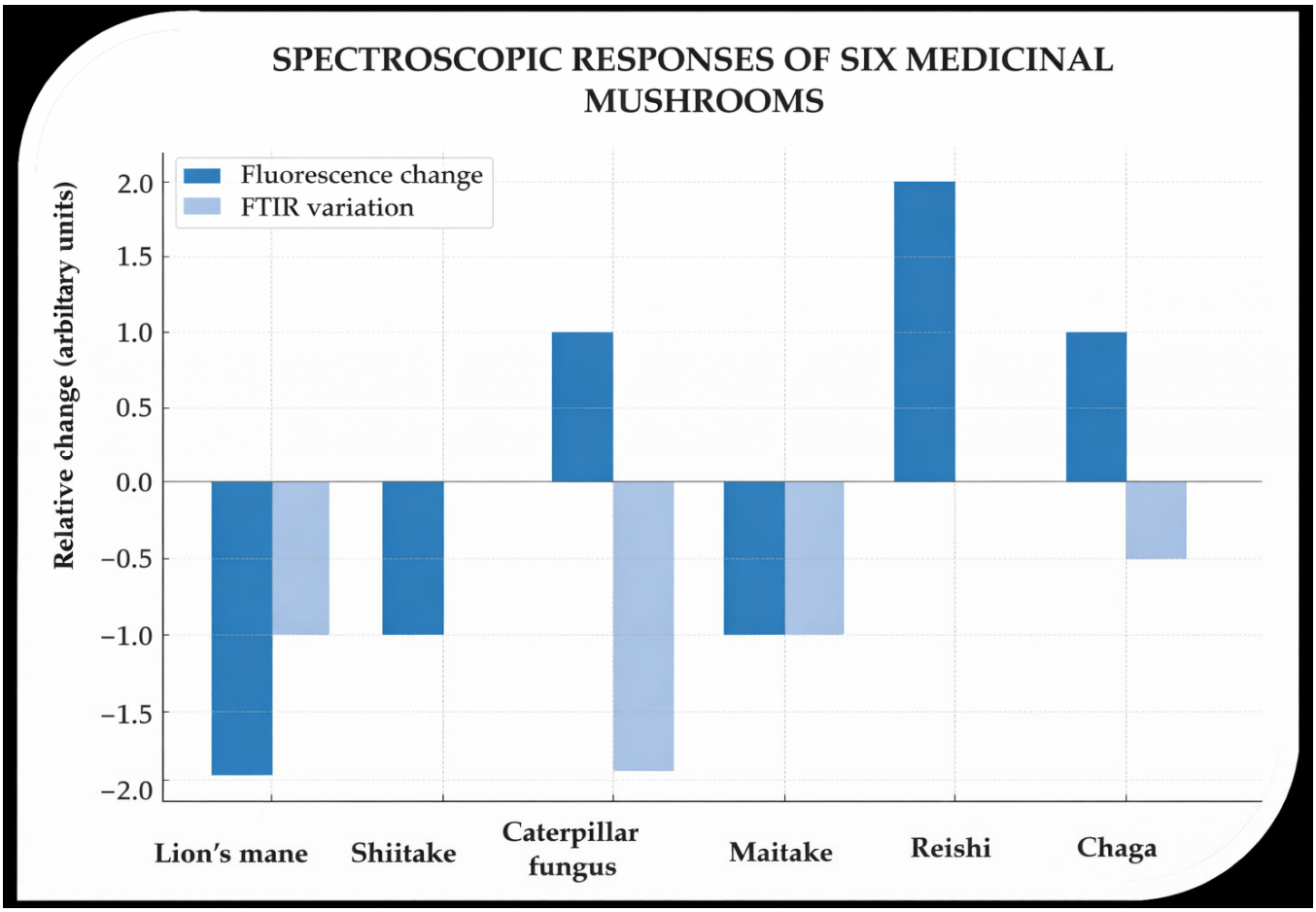

Figure 7. Relative changes in fluorescence intensity (dark blue) and FTIR spectral features (light blue) of six medicinal mushroom species after mild thermal treatment (200 °C, 3 h). Data illustrate species-dependent variations in the response to thermal processing, with most mushrooms showing increased fluorescence, whereas Cordyceps sinensis (caterpillar fungus) and Lion's mane show decreased fluorescence. FTIR variations indicate structural modifications in the polysaccharide and protein components. β-Glucan was not directly measured in the fluorescent fractions but serves as a compositional marker of the original mushroom matrix, potentially influencing the observed differences in thermal response.

Species-specific patterns are evident: *C. sinensis* and Lion's mane show the greatest alterations, reflecting significant molecular rearrangements and fluorophore transformations. In contrast, *G. lucidum* and *L. edodes* exhibit minimal changes, demonstrating high thermal resilience. *G. frondosa*, *H. erinaceus*, and *I. obliquus* display intermediate responses, consistent with partial dehydration, oxidation, and structural reorganization.

The combination of fluorescence and FTIR metrics proposes that mild thermal treatment induces measurable carbonization, while preserving core polysaccharide frameworks. It should be mentioned that fluorescence indicates the formation of nanoscale carbon domains through excitation-dependent emission, while FTIR reveals concurrent chemical

changes (e.g., dehydration and emergence of aromatic C=C bonds), together supporting incipient carbonization at the nanoscale. Correlation with β-glucan content (Tables 2 and 3) suggests that initial polysaccharide abundance and structural order influence the extent of thermal modification: species with higher or more ordered β-glucan maintain structural integrity, whereas species with moderate or less ordered glucans undergo greater molecular rearrangements, facilitating enhanced fluorescence.

Figure 7 highlights the species-dependent nature of thermal responses in medicinal mushrooms and underscores the critical role of β-glucan matrices in modulating mild thermal treatment-driven carbonaceous fractions synthesis.

β-Glucan content serves as a structural biomarker, providing insight into the molecular effects of mild thermal treatment observed via FTIR and fluorescence analyses. Mushrooms with higher initial β-glucan content, such as *G. lucidum*, exhibit greater thermal stability, as reflected by minimal FTIR spectral changes, likely due to polysaccharide-mediated protection of the cellular matrix. In contrast, species like *C. sinensis* and *H. erinaceus*, which have moderate baseline β-glucan levels and show pronounced spectral changes, display higher thermal lability, resulting in enhanced fluorophore transformation and oxidation.

Chaga (*I. obliquus*) and Maitake (*G. frondosa*) exhibited moderate structural rearrangements, yet both demonstrated an apparent increase in β-glucan content after mild thermal treatment. This increase is likely attributable to relative concentration effects from water loss or enhanced polysaccharide accessibility, potentially due to the unmasking of previously inaccessible β-glucan chains.

Notably, the observed fluorescence enhancement in *G. lucidum* and *I. obliquus*, despite minor FTIR changes, indicates the formation of new conjugated structures. These modifications may involve interactions between β-glucans and thermally altered aromatic residues, contributing to the generation of fluorescent carbonaceous fractions. The summarized β-glucan content for all species is presented in Table 4.

Table 4. Summarization of the results for β-glucan content.

Mushroom Species	β-Glucan Content (% *w*/*w*)	
	Commercially Available Mushroom Powder	Mild-Thermal Processed Mushroom Powder
Lion's mane	30.79 ± 2.83	37.1 ± 0.57
Shiitake	36.2 ± 3.04	47.1 ± 2.37
Caterpillar fungus	26.8 ± 0.99	29.6 ± 2.02
Maitake	36.3 ± 1.06	36.7 ± 0.57
Reishi	54.2 ± 10.04	36.6 ± 1.80
Chaga	28.1 ± 1.81	36.7 ± 0.64

4. General Discussion and Future Recommendations

The study investigates water-soluble fluorescent carbonaceous fractions formed during mild thermal treatment (200 °C, 3 h) of β-glucan-rich mushrooms. It does not claim the presence of carbon nanodots, as their confirmation would require nanoscale imaging and additional purification. The aim of the work is not process optimization, but the characterization of thermally induced fluorescent products in mushroom matrices. The synthesis of fluorescent carbon-based structures from medicinal mushrooms has attracted increasing attention due to their potential optical functionality, biocompatibility, and sustainable origin [26,27].

The inherent bioactive compounds in mushrooms, such as β-glucans and antioxidants, contribute to the formation, stability, and surface chemistry of carbonaceous fractions,

influencing their physicochemical and biological properties [28]. Moreover, mild thermal treatment temperatures around 200 °C provide sufficient thermal energy to induce carbonization while preserving certain functional groups, resulting in carbonaceous fractions with desirable fluorescence and chemical properties. Controlled mild thermal treatments enable environmentally friendly, scalable synthesis of fluorescent carbon materials with tunable surface chemistry, high quantum yield, and built-in functionality, often outperforming harsher conventional synthetic routes in sustainability and application-readiness [29,30].

The molecular profiling of mushroom powders revealed that pyrolytic processing, under the applied conditions, did not result in statistically significant changes in weight-average molecular weight (Mw), number-average molecular weight (Mn), or polydispersity index (PD%) across the studied species. These findings indicate that the main macromolecular structures remained largely intact following mild thermal treatment, with no detectable degradation or aggregation.

Significant increases ($p < 0.05$) were observed in most species after mild thermal treatment, with the notable exception of caterpillar fungus (*C. sinensis*), where fluorescence decreased substantially. This suggests that mild thermal treatment can enhance fluorescent behavior through dehydration, aromatization, and the formation of conjugated sp^2 domains that favor radiative recombination. However, in the case of *C. sinensis*, the comparatively higher protein and nitrogen-rich small-molecule content may promote alternative carbonization pathways leading to excessive crosslinking, formation of non-radiative defect sites, or over-carbonization. Such processes can reduce surface emissive traps and increase non-radiative recombination, resulting in fluorescence quenching. Therefore, species-specific biochemical composition appears to critically influence the balance between emissive domain formation and defect-induced quenching.

Our previous study has shown that mild thermal treatment usually preserves or only slightly alters size distributions while improving optical properties. For instance, carbonaceous fractions obtained from *P. ostreatus* maintained strong fluorescence and low polydispersity across different heating conditions, with only moderate changes in size profiles [6].

Because the changes in molecular weight and dispersity did not reach statistical significance in most comparisons, caution must be exercised in interpreting homogenization as a robust effect. Further studies employing larger sample sizes, multiple mild thermal treatment conditions (e.g., varying temperature and duration), and complementary characterization techniques (e.g., size-exclusion chromatography, TEM, Raman) are needed. Additionally, a mechanistic investigation (e.g., chemical fragmentation pathways, crosslinking dynamics) would better clarify how mild thermal treatment shapes the molecular architectures underlying fluorescence changes.

The mild thermal treatment process (P samples) significantly altered the fluorescence of all mushroom powders. A notable decrease in the emission maximum around 400 nm indicated the degradation or oxidation of protein- and phenolic-based fluorophores. In some samples, a slight red shift and spectral broadening (600–740 nm) suggested the formation of more conjugated, melanin-like structures via thermal polymerization. Overall, mild thermal treatment reduced fluorescence intensity but triggered structural changes in fluorophores, reflecting both degradation and recombination of aromatic and polyphenolic compounds. These spectral changes, diminished blue emission and a weak red shoulder, align with known photophysical behavior of heat-treated biopolymers and pigments [31]. The variations observed across species highlight the influence of the biochemical composition of the mushroom matrix, including β-glucan content, protein association, and phenolic profiles, on the stability, formation, and optical characteristics of water-soluble fluorescent carbonaceous fractions. The observed increase in fluorescence for most species

likely reflects the formation of conjugated sp^2 domains from mild thermal treatment, enhancing radiative recombination, whereas the decrease in *Cordyceps sinensis* is attributed to higher protein and nitrogen content promoting non-radiative defect formation and over-carbonization. The new band observed in the *Ganoderma lucidum* P sample is explained by the formation of more conjugated, melanin-like structures via partial thermal polymerization and aromatization of polyphenolic compounds.

The FTIR analysis indicates that mild thermal treatment at 200 °C for 3 h induces varying degrees of chemical alterations depending on the mushroom species. *C. sinensis* undergoes the most pronounced chemical transformations, which include dehydration, degradation of alkyl groups, and the formation of new carbonyl functionalities. In contrast, other species, such as *Ganoderma lucidum*, demonstrate remarkable thermal resilience, showing minimal changes under the same conditions. Species such as *G. frondosa*, *H. erinaceus*, *I. obliquus*, and *L. edodes* undergo only mild to moderate dehydration and modifications to functional groups, while retaining significant structural features. These findings highlight the importance of considering species-specific chemical composition and structural stability when assessing thermal processing methods, such as mild thermal treatment. Furthermore, among the tested mushroom species, *reishi* and *shiitake* serve as suitable controls for evaluating β-glucan stability, as they exhibited minimal FTIR spectral changes, suggesting limited structural degradation during pyrolytic processing. In contrast, caterpillar fungus and Lion's mane represent ideal candidates for studying the relationship between β-glucan degradation and changes in fluorophore composition, as both showed pronounced FTIR variations and significant shifts in fluorescence intensity, indicating substantial molecular transformation.

The observed FTIR modifications, when considered together with the unchanged Mw and Mn values, indicate that the applied treatment does not result in extensive or bulk carbonization. Instead, heating at 200 °C may induce partial carbonization, possible formation of carbon-rich domains, or structural rearrangements rather than complete carbonization. Furthermore, relative changes (Δ%) in baseline-corrected FTIR peak ratios after mild thermal treatment (Original → P) further support these observations, and these findings indicate that heating at 200 °C promotes partial structural reorganization and possible formation of carbon-rich domains without complete carbonization, supporting the generation of modified carbon-based structures while maintaining the overall macromolecular framework.

These findings highlight that species-specific β-glucan structure and branching patterns strongly influence thermal response and fluorescence outcomes. Mushrooms with highly ordered β-(1→3)-glucan backbones and limited side-branching, such as reishi and shiitake, exhibit minimal degradation and serve as useful controls for β-glucan stability under mild thermal treatment. Conversely, species with more amorphous or protein-associated glucans, such as caterpillar fungus and Lion's mane, show substantial FTIR and fluorescence changes, suggesting extensive molecular rearrangement.

In addition, hydroxyl and oxygen-containing groups from β-glucan precursors enable surface modification for imaging or drug delivery, consistent with biomass-derived carbon dots, where surface functionalities govern optical and catalytic properties [32]. Controlled carbonization also critically affects fluorescence and stability, underscoring the role of precursor composition and thermal conditions [33].

Future investigations should focus on quantifying the relationship between β-glucan degradation kinetics and fluorophore formation, potentially integrating thermogravimetric and spectroscopic analyses to map structural evolution during carbonization. A systematic correlation between mass loss profiles, chemical transformation pathways, and emission characteristics would provide mechanistic insight into the origin of fluorescence centers.

Overall, even mild thermal treatment of β-glucan-rich mushrooms can induce measurable photophysical and structural changes in water-soluble carbonaceous fractions, while largely preserving the polysaccharide framework. Species-specific glucan structure and protein content govern the extent of rearrangement and fluorescence outcomes. These insights provide a foundation for designing mushroom-derived materials with targeted optical or functional properties, bridging natural bioactive matrices and emerging applications in functional foods, nutraceuticals, and fluorescent fractions.

5. Conclusions

Mild thermal treatment (200 °C, 3 h) induced species-dependent chemical and photophysical modifications in β-glucan-rich medicinal mushroom powders. HPLC-SEC analysis indicated that the overall macromolecular size distributions (Mw, Mn, dispersity) remained largely unchanged, suggesting preservation of the principal polysaccharide framework under the applied conditions. In contrast, fluorescence and FTIR analyses revealed measurable functional-group alterations and intensity redistribution in the resulting water-soluble fluorescent carbonaceous fractions, consistent with partial dehydration and localized carbon-rich domain formation. These findings indicate controlled structural reorganization without extensive bulk degradation. The present study does not claim the isolation of discrete carbon dots; confirmation of nanoscale morphology requires dedicated imaging and purification. Further optimization and nanoscale characterization will clarify structure–property relationships and potential applications.

Author Contributions: Conceptualization and writing of the original draft, G.T.; sample preparation, G.T.; experimental analysis, G.T., R.A., D.S., A.F. and F.A.T.; visualization, R.A., D.S., A.F., J.P., F.A.T. and P.T.N.; data validation, G.T., R.A., A.F., D.S. and P.T.N.; revision, J.P., F.A.T. and P.T.N.; supervision, J.P. All authors have read and agreed to the published version of the manuscript.

Funding: This research was supported by the University of Debrecen Scientific Research Bridging Fund (DETKA) and by the University of Debrecen Program for Scientific Publication. The Doctoral Research Scholarship, EKÖP-25-3-II-DE-4 also funded the study.

Institutional Review Board Statement: Not applicable.

Informed Consent Statement: Not applicable.

Data Availability Statement: The original contributions presented in this study are included in the article. Further inquiries can be directed to the corresponding author.

Acknowledgments: The authors thank the three anonymous referees for their constructive comments on an earlier version of this manuscript.

Conflicts of Interest: The authors declare no competing interests.

References

1. Ahmed, A.; Shahadat, M.; Islam, S.U.; Adnan, R.; Mohamad Ibrahim, M.N.; Ullah, Q. Synthesis, Characterization, and Properties of Green Carbon Nanodots. In *ACS Symposium Series*; Islam, S.U., Hussain, C.M., Eds.; American Chemical Society: Washington, DC, USA, 2023; Volume 1441, pp. 25–39.
2. Acay, H.; Güler Güney, İ.; Yildirim, A.; Derviş, S.; Dereli, E. Green Synthesis of Pleurotus Eryngii-Derived Nanomaterials for Phytopathogen Control. *Chem. Biodivers.* **2024**, *21*, e202401972. [CrossRef] [PubMed]
3. Afonso, A.G., Jr.; Aquino, F.T.; Dalmônico, G.M.L.; Nascimento, M.V.; Wrasse, E.; De Aguiar, K.M.F.R. Green Synthesis of Carbon Nanodots from Agro-Industrial Residues. *Carbon Lett.* **2022**, *32*, 131–141. [CrossRef]
4. Chaudhari, V.; Vairagade, V.; Thakkar, A.; Shende, H.; Vora, A. Nanotechnology-Based Fungal Detection and Treatment: Current Status and Future Perspective. *Naunyn-Schmiedeberg's Arch. Pharmacol.* **2024**, *397*, 77–97. [CrossRef]
5. Owaid, M.N.; Ibraheem, I.J. Mycosynthesis of Nanoparticles Using Edible and Medicinal Mushrooms. *Eur. J. Nanomed.* **2017**, *9*, 5–23. [CrossRef]

6. Törős, G.; Béni, Á.; Balláné, A.K.; Semsey, D.; Ferroudj, A.; Prokisch, J. Production of Myco-Nanomaterial Products from Pleurotus Ostreatus (Agaricomycetes) Mushroom via Pyrolysis. *Pharmaceutics* **2025**, *17*, 591. [CrossRef]
7. Semsey, D.; Nguyen, D.H.H.; Törős, G.; Papp, V.; Pénzes, J.; Vida, T.; Béni, Á.; Rai, M.; Prokisch, J. Analysis of Fluorescent Carbon Nanodots Synthesized from Spices Through Thermal Processes Treatment. *Nanomaterials* **2025**, *15*, 625. [CrossRef] [PubMed]
8. Wei, W.; Xu, C.; Wu, L.; Wang, J.; Ren, J.; Qu, X. Non-Enzymatic-Browning-Reaction: A Versatile Route for Production of Nitrogen-Doped Carbon Dots with Tunable Multicolor Luminescent Display. *Sci. Rep.* **2014**, *4*, 3564. [CrossRef]
9. Cho, S.; Kim, H.; Song, D.; Jung, J.; Park, S.; Jo, H.; Seo, S.; Han, C.; Park, S.; Kwon, W.; et al. Insights into Glucose-Derived Carbon Dot Synthesis via Maillard Reaction: From Reaction Mechanism to Biomedical Applications. *Sci. Rep.* **2024**, *14*, 31325. [CrossRef]
10. Atta-Allah, A.A.; Ahmed, R.F.; Shahin, A.A.M.; Hassan, E.A.; El-Bialy, H.A.-A.; El-Fouly, M.Z. Optimizing the Synthesis of Yeast Beta-Glucan via Response Surface Methodology for Nanotechnology Application. *BMC Microbiol.* **2023**, *23*, 110. [CrossRef]
11. Cerletti, C.; Esposito, S.; Iacoviello, L. Edible Mushrooms and Beta-Glucans: Impact on Human Health. *Nutrients* **2021**, *13*, 2195. [CrossRef] [PubMed]
12. Cox, C.M.; Dalloul, R.A. Beta-Glucans as Immunomodulators in Poultry: Use and Potential Applications. *Avian Biol. Res.* **2010**, *3*, 171–178. [CrossRef]
13. Bohn, J.A.; BeMiller, J.N. (1→3)-β-d-Glucans as Biological Response Modifiers: A Review of Structure-Functional Activity Relationships. *Carbohydr. Polym.* **1995**, *28*, 3–14. [CrossRef]
14. Baker, S.N.; Baker, G.A. Luminescent Carbon Nanodots: Emergent Nanolights. *Angew. Chem. Int. Ed.* **2010**, *49*, 6726–6744. [CrossRef] [PubMed]
15. Li, H.; Kang, Z.; Liu, Y.; Lee, S.-T. Carbon Nanodots: Synthesis, Properties and Applications. *J. Mater. Chem.* **2012**, *22*, 24230. [CrossRef]
16. Titirici, M.-M.; Antonietti, M. Chemistry and Materials Options of Sustainable Carbon Materials Made by Hydrothermal Carbonization. *Chem. Soc. Rev.* **2010**, *39*, 103–116. [CrossRef]
17. Sevilla, M.; Fuertes, A.B. The Production of Carbon Materials by Hydrothermal Carbonization of Cellulose. *Carbon* **2009**, *47*, 2281–2289. [CrossRef]
18. Díez-Pascual, A.M. Carbon-Based Nanomaterials. *Int. J. Mol. Sci.* **2021**, *22*, 7726. [CrossRef]
19. El Sheikha, A.F.E. Nutritional Profile and Health Benefits of Ganoderma Lucidum "Lingzhi, Reishi, or Mannentake" as Functional Foods: Current Scenario and Future Perspectives. *Foods* **2022**, *11*, 1030. [CrossRef]
20. Zhuang, C.; Wasser, S.P. Medicinal Value of Culinary-Medicinal Maitake Mushroom Grifola Frondosa (Dicks.:Fr.) S.F. Gray (Aphyllophoromycetideae). Review. *Int. J. Med. Mushrooms* **2004**, *6*, 287–314. [CrossRef]
21. Chen, P.X.; Wang, S.; Nie, S.; Marcone, M. Properties of Cordyceps Sinensis: A Review. *J. Funct. Foods* **2013**, *5*, 550–569. [CrossRef]
22. Balandaykin, M.E.; Zmitrovich, I.V. Review on Chaga Medicinal Mushroom, Inonotus Obliquus (Higher Basidiomycetes): Realm of Medicinal Applications and Approaches on Estimating Its Resource Potential. *Int. J. Med. Mushrooms* **2015**, *17*, 95–104. [CrossRef] [PubMed]
23. Ahmad, I.; Arif, M.; Mimi, X.; Zhang, J.; Ding, Y.; Lyu, F. Therapeutic Values and Nutraceutical Properties of Shiitake Mushroom (Lentinula Edodes): A Review. *Trends Food Sci. Technol.* **2023**, *134*, 123–135. [CrossRef]
24. Nguyen, D.H.H.; Muthu, A.; El-Ramady, H.; Daróczi, L.; Nagy, L.; Kéki, S.; Béni, Á.; Csarnovics, I.; Prokisch, J. Optimization of Extraction Conditions to Synthesize Green Carbon Nanodots Using the Maillard Reaction. *Mater. Adv.* **2024**, *5*, 3499–3505. [CrossRef]
25. McCleary, B.V.; Draga, A. Measurement of β-Glucan in Mushrooms and Mycelial Products. *J. AOAC Int.* **2016**, *99*, 364–373. [CrossRef]
26. Duan, Q.; He, Y.; Long, X.; Wang, J.; Ni, C.; Wu, S. Synthesis of Green Photoluminescence Carbon Dots Using Edible Seafood Mushroom and Their Anti-Counterfeiting Applications. *Adv. Sustain. Syst.* **2024**, *8*, 2300536. [CrossRef]
27. Venkatesan, P.; Govindasamy, R.; Periyasami, G.; Rahaman, M.; Pandiaraj, S.; Thiruvengadam, M.; Thirumalaivasan, N.; Wu, S.-P. Eco-Friendly, Bright Luminescent Carbon Dots and Their Potential Applications for Detecting Hypochlorous Acid in Water and Live Cell Imaging. *J. Mater. Res. Technol.* **2023**, *24*, 6522–6532. [CrossRef]
28. Törős, G.; El-Ramady, H.; Nguyen, D.H.H.; Alibrahem, W.; Kharrat Helu, N.; Atieh, R.; Muthu, A.; Jevcsák, S.; Semsey, D.; Abdalla, N.; et al. Green-Synthesized Nanomaterials from Edible and Medicinal Mushrooms: A Sustainable Strategy Against Antimicrobial Resistance. *Pharmaceutics* **2025**, *17*, 1388. [CrossRef]
29. Liu, X.; Li, H.-B.; Shi, L.; Meng, X.; Wang, Y.; Chen, X.; Xu, H.; Zhang, W.; Fang, X.; Ding, T. Structure and Photoluminescence Evolution of Nanodots During Pyrolysis of Citric Acid: From Molecular Nanoclusters to Carbogenic Nanoparticles. *J. Mater. Chem. C* **2017**, *5*, 10302–10312. [CrossRef]
30. Gümrükçüoğlu, A.; Ocak, M.; Kolaylı, S.; Dinç, S.; Altin, I.; Gün, S.; Turgut Ocak, Ü. Spectrofluorometric Determination of Fe^{3+}, Pd^{2+}, and Sn^{2+} Ions Using Carbon Nanodots Derived from Hazelnut Shells. *Methods Appl. Fluoresc.* **2025**, *13*, 035002. [CrossRef]
31. Radotić, K.; Stanković, M.; Bartolić, D.; Natić, M. Intrinsic Fluorescence Markers for Food Characteristics, Shelf Life, and Safety Estimation: Advanced Analytical Approach. *Foods* **2023**, *12*, 3023. [CrossRef] [PubMed]

32. Xu, J.; Chen, Y.; Zhang, S.; Zhu, H.; Mao, Z.; Lin, Z.; Chen, Z.; Lian, H.; Gao, L.; Li, Y. Aqueous-Stable Perovskite Nanoprobes via Dual-Anchoring Strategy for Sensitive Tumor-Associated Phospholipase D Biosensing. *Chem. Eng. J.* **2026**, *528*, 172365. [CrossRef]
33. Satria, M.; Alarifi, M.; Hardianto, Y.P.; Saleh, T.A. Sustainable Carbon Quantum Dots from Biomass for Fluorescence and Acidic Hydrogen Evolution. *ACS Sustain. Resour. Manag.* **2026**, *3*, 733–747. [CrossRef]